

PARADIGM SHIFT OF THE PLASMA MEMBRANE CONCEPT FROM THE TWO-DIMENSIONAL CONTINUUM FLUID TO THE PARTITIONED FLUID: High-Speed Single-Molecule Tracking of Membrane Molecules

Akihiro Kusumi, Chieko Nakada, Ken Ritchie,
Kotono Murase, Kenichi Suzuki, Hideji Murakoshi,
Rinshi S. Kasai, Junko Kondo, and Takahiro Fujiwara
*Kusumi Membrane Organizer Project, Exploratory Research for Advanced Technology
Organization (ERATO/SORST-JST), Department of Biological Science and Institute for
Advanced Research, Nagoya University, Nagoya 464-8602, Japan;
email: akusumi@bio.nagoya-u.ac.jp*

Key Words plasma membrane compartments, actin-based membrane-skeleton
fence model, anchored-transmembrane protein pickets, single-particle tracking,
single fluorescent molecule video imaging

■ **Abstract** Recent advancements in single-molecule tracking methods with nano-meter-level precision now allow researchers to observe the movement, recruitment, and activation of single molecules in the plasma membrane in living cells. In particular, on the basis of the observations by high-speed single-particle tracking at a frame rate of 40,000 frames s^{-1} , the partitioning of the fluid plasma membrane into submicron compartments throughout the cell membrane and the hop diffusion of virtually all the molecules have been proposed. This could explain why the diffusion coefficients in the plasma membrane are considerably smaller than those in artificial membranes, and why the diffusion coefficient is reduced upon molecular complex formation (oligomerization-induced trapping). In this review, we first describe the high-speed single-molecule tracking methods, and then we critically review a new model of a partitioned fluid plasma membrane and the involvement of the actin-based membrane-skeleton “fences” and anchored-transmembrane protein “pickets” in the formation of compartment boundaries.

CONTENTS

INTRODUCTION	352
OVERVIEW OF THIS REVIEW	353

TWO FUNDAMENTAL PROBLEMS: OBSERVATIONS THAT CANNOT BE EXPLAINED BY THE SINGER-NICOLSON FLUID MOSAIC MODEL OR THE TWO-DIMENSIONAL CONTINUUM FLUID MODEL	354
NO SIMPLE BROWNIAN DIFFUSION IN THE PLASMA MEMBRANE	356
Lipid Molecules Undergo Hop Diffusion in the Plasma Membrane	
But Not in Liposomes	356
Lipid Diffusion within a Compartment is Simple Brownian, Similar to that Found in Liposomes	358
A Paradigm Shift of the Plasma Membrane Structure Concept May Be Necessary ..	358
Apparent Simple Brownian Diffusion Occurs in Limited Time Windows	359
Why Is Hop Diffusion of Membrane Molecules Generally Missed?	361
Plasma Membrane Compartmentalization is Universally Found	
Among Mammalian Cells in Culture	361
THE MEMBRANE-SKELETON FENCE MODEL AND THE ANCHORED-TRANSMEMBRANE PROTEIN PICKETS MODEL	362
Both Membrane Proteins and Lipids Undergo Hop Diffusion in the Partitioned Plasma Membrane	362
The Membrane-Skeleton Fence Model for Temporary Corralling of Transmembrane Proteins	363
The Model of Anchored-Transmembrane Protein Pickets, Which Work for All the Membrane Molecules in the Plasma Membrane	364
OLIGOMERIZATION-INDUCED TRAPPING	366
A PARADIGM SHIFT OF THE LONG-RANGE STRUCTURE OF THE CELL MEMBRANE	368
A Paradigm Shift from the Two-Dimensional Continuum Fluid to the Compartmentalized Fluid	368
Other Related Observations and Models Regarding the Reduction of Diffusion Coefficients in the Plasma Membrane Compared to Those in Artificial/Reconstituted Membranes	368
Summary of the Evidence Supporting the Membrane-Skeleton Fence and Anchored-Transmembrane Protein Picket Models for Compartmentalization of the Cell Membrane	370
DEVELOPMENTAL FORMATION OF A DIFFUSION BARRIER IN THE NEURONAL INITIAL SEGMENT CELL MEMBRANE	372
CONCLUSIONS	373

INTRODUCTION

We first introduce the readers to the high-temporal-resolution (25- μ s) trajectories of an unsaturated phospholipid L- α -dioleoylphosphatidylethanolamine (DOPE) tagged with a colloidal gold particle 40 nm in diameter (Figure 1a, see color insert). DOPE is an unsaturated phospholipid, and thus it is considered one of the most resistant molecular species to various mechanisms for reducing the diffusion rate, such as the presence of integral membrane proteins and cholesterol (40). To observe DOPE movement, it was tagged with a fluorescent dye, Cy3, or a colloidal gold particle with a diameter of 40 nm. In our video-rate observations (a resolution of

33 ms, and in a time window of approximately 100 ms), both gave similar diffusion coefficients, which justifies the use of such a large colloidal gold particle as a probe, as long as we remained in time windows shorter than 100 ms. The technical details are given in Box 1 (also see Box 2 for the early history of single-molecule tracking in the live cell membrane). (Because of space limitations, we refer readers to Box 1 through Box 8, which describe further important points related to the main text and are provided as Supplemental Material; follow the Supplemental Material link from the Annual Reviews home page at <http://www.annualreviews.org/>).

At an enhanced time resolution of 25 μs (or a frame rate of 40,500 frames s^{-1} , 1350 times faster than the normal video rate), virtually all the colloidal-gold-tagged DOPE molecules (Gold-DOPE) on the cell surface exhibited characteristic trajectories that strongly amazed us when we first saw them: The DOPE molecules appeared to undergo short-term confined diffusion within a compartment and long-term hop movement between the compartments, which we call “hop diffusion” (18) (Figure 1*a*). This was unexpected, based on previously established models such as the fluid mosaic model by Singer & Nicolson (69) and the two-dimensional continuum fluid model of Saffman & Delbrück (45) (our initial idea was to find lipid raft domains using various lipid probes, by observing them at high time resolutions; DOPE, a typical nonraft lipid, was our first control sample). Our initial statistical analysis of these high-definition trajectories showed that virtually all the obtained trajectories of DOPE were of the hop-diffusion type (at least non-Brownian long-term suppressed diffusion) (Figures 1 and 2, see color insert). This was not observed at observation rates slower than the hop rate (Figure 1*b*) nor in liposomes even at a resolution of 25 μs (Figure 1*c*). These results instantly led us to a working hypothesis addressing why the diffusion in the plasma membrane is slower than that found in liposomes or reconstituted membranes by factors of 5 to 50, a thirty-year-old enigma in the field of membrane biophysics: The plasma membrane is partitioned with regard to molecular diffusion because of the interactions with the membrane skeleton.

OVERVIEW OF THIS REVIEW

In this article, we first summarize two critical previous observations (although many examples exist) that cannot be explained by the Singer-Nicolson fluid mosaic model or the Saffman-Delbrück two-dimensional continuum fluid model. We then review the various results obtained by high-speed single-molecule tracking of the phospholipid molecule, DOPE, including its technical problems, solutions, and the consistency of the results with previous observations, which involve averaging over many molecules, long time windows, or both.

Third, we present various models that address how the diffusion in the cell membrane may be suppressed, including earlier models as well as more recent ones we proposed: the plasma membrane compartmentalization model, the membrane-skeleton fence and anchored-transmembrane protein picket models, and the

oligomerization-induced trapping model. We test these models against a variety of experimental observations, emphasizing the importance of examining all the related observations rather than only analyzing the diffusion data, in particular those averaged over many molecules. In the end, we hope to persuade the readers to think of the plasma membrane as a compartmentalized fluid, in which compartmentalization is caused by the fence (corralling) effects of the membrane skeleton as well as the hydrodynamic slowing effects of transmembrane-protein pickets anchored on the membrane-skeleton fence. In addition, we hope that the readers will become interested in high-speed single-molecule tracking techniques and their applications to the plasma membrane research.

TWO FUNDAMENTAL PROBLEMS: OBSERVATIONS THAT CANNOT BE EXPLAINED BY THE SINGER-NICOLSON FLUID MOSAIC MODEL OR THE TWO-DIMENSIONAL CONTINUUM FLUID MODEL

There have been two major long-standing problems regarding the two-dimensional continuum fluid model of the plasma membrane, which is based on the Singer-Nicolson fluid mosaic model (41, 45, 69). For 30 years, membrane biologists wondered why the diffusion coefficients for both proteins and lipids in the plasma membrane are smaller than those found in artificially reconstituted membranes or liposomes by factors of 5 to 50. In Table 1 the diffusion coefficients of various membrane proteins in reconstituted membranes are compared with those of the plasma membrane. The diffusion coefficients of a variety of lipid probes and glycosylphosphatidylinositol (GPI)-anchored proteins observed in artificial membranes as well as in the cell membrane are listed in supplemental Table S1 (follow the Supplemental Material link from the Annual Reviews home page at <http://www.annualreviews.org/>). Note that the diffusion coefficients in these displays represent the “macroscopic” diffusion coefficients, which generally refer to the diffusion coefficients in space scales greater than several hundred nanometers, corresponding to the typical photobleaching area size in the fluorescence redistribution after photobleaching (FRAP) experiments or to the compartment size (30 to 230 nm, depending on the cell type) (Figure 3*b*, see color insert) in the compartmentalized (or partitioned) membrane model. Various models have been proposed to explain this large difference in the macroscopic diffusion coefficients between plasma membranes and artificial/reconstituted membranes; however, no consensus has been reached (see below).

Second, when membrane molecules, including receptor molecules and other signaling molecules in the plasma membrane, form oligomers or molecular complexes, their diffusion rates drop dramatically or they may be temporarily immobilized (22, 38, 44). Furthermore, the macroscopic diffusion coefficient of the transmembrane protein E-cadherin was decreased by a factor of 40 upon oligomerization (including various sizes of clusters ranging from dimers to perhaps

TABLE 1 Comparison of diffusion coefficients of the same (or similar) membrane proteins between artificial versus cellular plasma (*italic characters*) membranes

Probe-Protein ^a	Lipid for artificial membranes and the cell type ^b	Method	Mobile fraction (%)	Effective D (mean \pm SD) ($\mu\text{m}^2 \text{s}^{-1}$)	Time window for D (ms)	Temp. ($^{\circ}\text{C}$)	Reference
Fl-Integrin $\alpha\text{IIB}\beta 3$	DMPG:DMPC = 1:1	FRAP	57	0.70 (± 0.06)	~5000	33	15
<i>Fl-Fab-Integrin $\beta 1$</i>	<i>AG1518</i>	<i>FRAP</i>	67	0.058 (± 0.002)	3000	37	2
Fl-AchR	DMPC	FRAP	>95	2.4 (± 0.8)	2600	36	77
Rh-AchR	<i>Rat Myotube</i>	<i>FRAP</i>	75	0.016 (± 0.003)	44,000	37	4
Fl-Glycophorin ^{#1}	DMPC	FRAP	85 ~ 98	2	3000	30	78
Fl-Glycophorin ^{#1}	DMPC	FRAP	85 ~ 98	4 (± 2)	1500	30	25
<i>Fl-Glycophorin^{#2}</i>	<i>Erythrocyte (intact)</i>	<i>FRAP</i>	56	0.0036 (± 0.0017)	10,0000	37	20
<i>Fl-Glycophorin^{#2}</i>	<i>Erythrocyte (ghost)</i>	<i>FRAP</i>	98	0.047 (± 0.021)	10,000	37	20
Fl-Band3	DMPC	FRAP	98	1.6 (± 0.4)	600	30	7
<i>Eo-Band3</i>	<i>Erythrocyte (ghost)</i>	<i>FRAP</i>	60 ~ 79	7 ~ 14	21,000 ~ 43,000	30	21
<i>Fl-Band3</i>	<i>Erythrocyte (ghost)</i>	<i>FRAP</i>	40	0.60 (± 0.069)	26,000	26	76
<i>Gold-Band3</i>	<i>Erythrocyte (ghost)</i>	<i>SPT</i>	70	0.0066	400,1000	37	74
Fl-Thy-1	DOPC:SM = 1:1	FRAP	—	0.58 (± 0.04)	1500	24	12
<i>Gold-Thy-1</i>	C3H 10T1/2	<i>SPT</i>	28	0.081 (± 0.007)	<6600	37	62

^aFl-Integrin $\alpha\text{IIB}\beta 3$, fluorescein-isothiocyanate (FITC)-labeled integrin $\alpha\text{IIB}\beta 3$; Fl-Fab-Integrin $\beta 1$, FITC-labeled TS2/16 Fab fragment bound to integrin $\beta 1$; Fl- and Rho-AchR, fluorescein- and tetramethylrhodamine-labeled bungarotoxin bound to acetylcholine receptor, respectively; Fl-Glycophorin^{#1}, FITC-labeled glycophorin; Fl-Glycophorin^{#2}, fluorescein-thiosemicarbazide-labeled glycophorin; Fl-Band3, FITC-labeled band3; Eo-Band 3, Eosin-labeled band 3; Fl-Thy-1, FITC-labeled Thy-1.

^bDMPG, 1,2-dimyristoyl-sn-glycero-3-phosphoglycerol; DMPC, 1,2-dimyristoyl-sn-glycero-3-phosphocholine; AG1518, AG1518 human foreskin fibroblast; DOPC, 1,2-dioleoyl-sn-glycero-3-phosphocholine; SM, sphingomyelin; C3H 10T1/2, C3H 10T1/2 mouse embryo fibroblast.

oligomers containing several tens of monomers) in the plasma membrane (23). Even DOPE, upon artificial crosslinking, exhibited a macroscopic diffusion rate slowed by a factor of 5 (35). These results contrast with the general view of membrane biologists.

On the basis of the fluid mosaic model of Singer & Nicolson (69), Saffman & Delbrück (45) derived an equation that relates the diffusant size to the translational diffusion coefficient in a two-dimensional continuum fluid. For a cylinder (a transmembrane protein) of radius a and height h , floating in a two-dimensional fluid of viscosity μ with a matched thickness (h) immersed in an aqueous medium of viscosity μ' , the translational and rotational diffusion coefficients, D_T and D_R , respectively, for the cylinder can be expressed as

$$D_T = \frac{k_B T}{4\pi \mu h} \left(\log \frac{\mu h}{\mu' a} - \gamma \right) \quad 1.$$

$$D_R = \frac{k_B T}{4\pi \mu a^2 h}, \quad 2.$$

where γ is the Euler constant (≈ 0.5772). This equation predicts that translational diffusion is insensitive to the diffusant size. Tetramer formation from monomers (an increase in radius by a factor of 2) decreases the diffusion rate by only a factor of 1.1, and even 100 mers (an increase in radius by a factor of 10) have a diffusion rate reduced by only a factor of 1.4 from that of monomers, assuming that the monomer radius of the membrane-spanning domain is 0.5 nm. Thus, if one believes in the two-dimensional continuum fluid model for the plasma membrane on the macroscopic scale (over several tens of nanometers), then what the diffusion theory teaches us is that oligomerization or the formation of molecular complexes hardly reduces the diffusion rate (45). Thus, the great reduction of the diffusion coefficient, upon oligomerization or molecular complex formation, as described above, clearly indicates that the plasma membrane cannot be considered a two-dimensional continuum fluid.

Therefore, a new model is certainly required that can explain both (a) the much slower diffusion of membrane proteins and lipids in the cell membrane compared with that in artificial, reconstituted membranes, and (b) the great reduction of the diffusion coefficient or the immobilization upon oligomerization or molecular complex formation.

NO SIMPLE BROWNIAN DIFFUSION IN THE PLASMA MEMBRANE

Lipid Molecules Undergo Hop Diffusion in the Plasma Membrane But Not in Liposomes

For the successful observation of anomalous diffusion or hop diffusion of membrane molecules in the plasma membrane, temporal issues regarding the data

acquisition must be considered. These include (a) the frame exposure time (the exposure time for a single frame), (b) the frame acquisition rate, and (c) the total length of tracking a single molecule. These technically important points are summarized in Box 3.

Other methodological issues have been raised and addressed. These include (a) instrumental signal-to-noise ratios [17-, 6.9-, and 4.0-nm accuracy in the position determination in single-particle tracking (SPT) at 25- μ s, 2-ms, and 33-ms resolutions, respectively (18; T. Fujiwara, unpublished observation), and 33 nm for Alexa 633 and 52 nm for Cy3 in single fluorescent molecule video imaging (SFVI) at time resolutions of 33 and 5 ms, respectively (I. Koyama & C. Nakada, unpublished observations)], (b) labeling [the size of the gold probes, their nonspecific interactions with various molecules, and their crosslinking effect are addressed in Box 4, Q1, and here we only point out that the gold-probe data are consistent with previous FRAP and slow single-molecule data, as shown in Table S1, and that in membrane blebs, a balloon-like area where the membrane skeleton is scarce, the diffusion coefficient is comparable to that found in liposomal/reconstituted membranes], and (c) the statistical [in fact, the success of much single-molecule research depends on the development of good statistical methods to analyze the data (18, 31)] and quantitative analysis of the obtained trajectories (18, 31; Boxes 5 and 6).

Statistical and quantitative analyses of single-molecule trajectories are usually carried out on the basis of the plot of the mean-square displacement (MSD) against the time interval (31, 43) (Figure 2). Fujiwara et al. (18) evaluated the likelihood that such trajectories could be induced by simple thermal diffusion, and found that more than 85% of the DOPE molecules underwent nonrandom long-term suppressed diffusion, consistent with short-term confined diffusion within a compartment and long-term hop movement over various compartments (hop diffusion, Figure 3a). Using compartment detection software (see Box 5), the authors determined the membrane compartments sensed by the diffusing molecules (because the compartments are created owing to the partitioning of the plasma membrane, they collectively occupy the whole plasma membrane, but the locations of the individual compartment boundaries have to be determined for each compartment), and these are shown in various colors in the trajectories displayed in Figure 1a. These results indicate that the plasma membrane is partitioned into submicron-sized compartments with regard to the translational diffusion of lipid molecules (the model of plasma membrane compartmentalization, Figure 3a).

Quantitative analyses of individual DOPE trajectories for the evaluations of the compartment size, the macroscopic and microscopic diffusion coefficients representing those for free diffusion within a compartment and those due to hop movement over the compartments for long time ranges, and the calculation of the average hop frequency (or the average residency time within a compartment) of a particular Gold-DOPE complex were carried out by a computer program, again based on the MSD-t plot (Figure 2), using the theory by Powles et al. (42; see Box 6). Quantitative analyses (Figure 2) of the trajectories, such as those displayed in

Figure 1a, showed that the average compartment size was 230 nm, and the average residency time within each 230-nm compartment was 11 ms, in the case of normal rat kidney epithelial (NRK) cells (these values vary greatly depending on the cell type; see Figure 3b). It is no wonder that hop movement, which takes place every 11 ms on average, could not be detected by conventional video-rate observations with a time resolution of only 33 ms, as shown in Figure 1b.

Lipid Diffusion within a Compartment is Simple Brownian, Similar to that Found in Liposomes

The diffusion rate within the 230-nm compartment, which is $5.4 \mu\text{m}^2 \text{s}^{-1}$ on average, is interesting. Fujiwara et al. (18) observed DOPE diffusion in membrane blebs (balloon-like structures of the plasma membranes, where the membrane skeleton is largely lost, and they further reduced the actin-based membrane skeleton by treating cells with latrunculin) and in liposomes, and found that DOPE molecules undergo rapid, simple Brownian diffusion with a diffusion coefficient of $\approx 9 \mu\text{m}^2 \text{s}^{-1}$ in these membranes (see Figure 2 for the MSD-t plot). Therefore, the measured diffusion coefficient within a compartment ($5.4 \mu\text{m}^2 \text{s}^{-1}$) is approximately 40% smaller than that for free diffusion of DOPE in the membrane ($9 \mu\text{m}^2 \text{s}^{-1}$). This reduction is probably due to a lack of time resolution, because even at a frame time of $25 \mu\text{s}$, a molecule diffusing at a rate of $9 \mu\text{m}^2 \text{s}^{-1}$ would cover an area with 30-nm radius. Approximately half of the 230-nm compartment area is within 30 nm of the compartment boundaries, and the DOPE molecules in this area are likely to sense the presence of the boundary and to bounce off the wall. This would substantially decrease their MSDs, even for several frame times, leading to a lower observed microscopic diffusion coefficient within a compartment. Therefore, this reduction is probably due to experimental limitations rather than to molecular interactions in the plasma membrane.

A Paradigm Shift of the Plasma Membrane Structure Concept May Be Necessary

The results summarized above suggest that (a) the plasma membrane is compartmentalized with regard to the translational diffusion of phospholipids; (b) that the lipid molecules undergo short-term confined diffusion within a compartment and long-term hop diffusion between these compartments; (c) that it takes time to hop from a compartment to an adjacent one (Figure 3a), which slows the macroscopic diffusion of membrane molecules in the plasma membrane compared with those in liposomes or reconstituted membranes, which could explain the thirty-year-old enigma of why diffusion is slower in the plasma membrane than in artificial reconstituted membranes by factors of 5–50; and (d) that further smaller compartments within the smaller 230-nm compartment are not likely to exist in NRK cells because the diffusion coefficient within the 230-nm compartment is already as fast as that observed in liposomes.

The two-dimensional continuum fluid model (45), based on the fluid mosaic model of Singer & Nicolson (69), is not compatible with the hop diffusion observed above. In fact, these models are consistent with the finding made within a compartment, i.e., as long as the spatial scale is limited to the size of the original cartoon depicted by Singer & Nicolson (69) (although at the smaller limit of the molecular scale, the continuum model would also fail), which is approximately $10 \text{ nm} \times 10 \text{ nm}$, calculated based on the number of lipids in the figure (Figure 3a, inset). There, the lipid molecules basically diffuse freely, as dictated by the membrane viscosity, as suggested in these models. However, in spatial scales over several tens of nanometers in the plasma membrane, simple-minded extensions of the fluid mosaic model of Singer & Nicolson (69) and the continuum fluid theory by Saffman & Delbrück (45) fail. The cell appears to have developed (during evolution) the means to control the long-range diffusion of membrane molecules.

As such, a paradigm shift from the two-dimensional continuum fluid to the compartmentalized fluid may be required for the concept of a plasma membrane structure in spatial scales larger than 10 nm , in which its constituent molecules undergo hop diffusion over the compartments.

Apparent Simple Brownian Diffusion Occurs in Limited Time Windows

Diffusion anomaly is often discussed using the relationship: $\text{MSD} = Ct^\alpha$ ($0 \leq \alpha \leq 1$, $C = \text{constant}$), where α parameterizes the level of anomaly (17, 54). In the case of simple Brownian diffusion, $\alpha = 1$. For the sake of clear display, another plot, $\log(\text{MSD}/\text{time})$ versus $\log(\text{time})$ [$\log(\text{MSD}/\text{time}) = (\alpha - 1) \log(\text{time}) + C'$, $C' = \text{constant}$], has become a standard method. In this display, the plot becomes flat (the slope $\alpha - 1 = 0$) when $\alpha = 1$ (when the diffusion is simple Brownian) (17, 51, 54, 62, 68). When diffusion is anomalous, α becomes less than 1, giving the plot of $\log(\text{MSD}/\text{time})$ versus $\log(\text{time})$ a negative slope ($\alpha - 1 < 0$).

Figure 4 (see color insert) shows this plot for DOPE in cultured FRSK (fetal rat skin keratinocyte) cells in the time range covering approximately five orders of magnitude ($50 \mu\text{s}$ – 2 s) (18, 35). Similar results were obtained for the μ -opioid receptor, a G protein-coupled receptor, by K. Suzuki & A. Kusumi (unpublished observations). First, for DOPE molecules in membrane blebs in FRSK cells (Figure 4), the plot is almost flat, between $50 \mu\text{s}$ and 12 ms , when observed at a resolution of $25 \mu\text{s}$. The best fit for the plot yields a slope ($\alpha - 1$) of 0.012 ($\alpha \cong 1$), which indicates that DOPE in membrane blebs undergoes simple Brownian diffusion.

On the other hand, the plot for the normal cell membrane is not flat at all. Diffusion is certainly anomalous in the cell membrane (36, 49–51, 53, 54, 56–58). The plot can be fitted, assuming the presence of three characteristic time zones, with α values of 0.97 ($50 \mu\text{s}$ to 0.13 ms), 0.53 (1 to 10 ms), and 0.94 (300 ms to 2 s), i.e., with two transition points, one at $\sim 0.1 \text{ ms}$ (or less) and the other between

10 ms and 100 ms (Figure 4). The idea of the three time zones is based on the concept of the partitioned plasma membrane, in which the following molecular events might take place on different timescales: (a) the short time zone in which Gold-DOPE corralled inside 40-nm compartments does not sense the presence of compartment boundaries (flatter left end), undergoing pseudosimple Brownian diffusion (thereby $\alpha - 1 \approx 0$); (b) the medium time zone in which Gold-DOPE undergoes microscopic diffusion inside the compartment on short timescales, while occasionally hopping to adjacent compartments (the steep negative slope of $\alpha - 1 \approx -0.47$); and (c) the long time interval in which Gold-DOPE appears to undergo simple Brownian diffusion, hopping between compartments randomly (flattened end on the right, with $\alpha - 1 \approx 0$). The upper transition time (10–100 ms) is consistent with the average residency time (15 ms) obtained from the hop analysis (Box 6). Furthermore, the difference in these plots between intact and bleb membranes indicates the involvement of the membrane skeleton in the hop diffusion of DOPE, consistent with Tank et al. (72). This point is discussed in detail below.

The above discussion indicates that if we assume that DOPE undergoes hop diffusion in a compartmentalized plasma membrane, then we could explain the display shown in Figure 4. However, this does not mean that the partitioned fluid model is the only model that can explain this display. In fact, using a Monte Carlo simulation, Saxton showed that diffusion becomes anomalous in the presence of moderate concentrations of immobile obstacles (for an example, see figure 4b in Reference 54). The general shape of the plot for the case of multicenter diffusion-limited aggregates is similar to that for the intact FRSK cell membrane, shown in Figure 4. A better display than the plot of the mean $\log(\text{MSD}/\text{time})$ versus $\log(\text{time})$, such as that shown in Figure 4, is required, and this may be a place where physics-oriented membrane researchers could make a great contribution to membrane biophysics.

We took a different approach. We tried to understand the underlying mechanism that induces such a special type of (at least this is what we believed) anomalous diffusion, and by doing so, we tried to examine whether the partitioned fluid model for the plasma membrane is true. A variety of our examinations are summarized below as well as in Box 7. Here, we emphasize that, although many models for anomalous diffusion can easily be conceived, and some of them may be consistent with the general features of the plot of the mean $\log(\text{MSD}/\text{time})$ versus $\log(\text{time})$ shown in Figure 4, these models must be examined against all other related observations, such as those summarized below (pay special attention to Item 1 and Item 4 in Box 7, which most proposed models are often unable to explain). Without such critical examinations against all other existing data, in addition to the diffusion data, the models will not be useful for understanding the molecular events occurring in the plasma membrane. Furthermore, it is surprising that many researchers do not seem to pay attention to the individual trajectories of each molecule. It should be clearly realized that much information is lost in the process of making such displays, as shown in Figures 2 and 4.

Therefore, the bottom line to be understood in this section is that the molecules incorporated into the plasma membrane do not undergo simple Brownian diffusion, and therefore most of the present methods for observing membrane molecules' lateral diffusion measure only "effective diffusion coefficients" in space scales over 300 nm and in timescales over 100 ms. Researchers must understand that the rate of diffusion in the cell membrane cannot be described by a single diffusion coefficient (because the assumption of simple Brownian diffusion breaks down), and thus all the diffusion coefficients obtained by FRAP or those estimated by single-molecule techniques at slow rates (perhaps slower than 1 ms, such as video rate) must be thought of as the "effective diffusion coefficients." We still claim that these measurements are useful (and we carry out these measurements in our laboratory almost every day), but to make them useful, the involved time windows must be understood and explicitly specified in the literature (17, 18, 22, 30, 35, 55, 58, 80). This constitutes a major difference from simple Brownian diffusion cases, in which the observation time window should not matter, as taught in undergraduate physics courses.

Why Is Hop Diffusion of Membrane Molecules Generally Missed?

Consider again the flattened end of the plot in Figure 4 (right). This shows that if single-molecule data are obtained at time resolutions of 30 ms or longer, then only the flattened end on the right in such a plot may be observed, leading to the erroneous conclusion that the molecule undergoes simple Brownian diffusion.

In the interpretation of the FRAP data or the results obtained by single-molecule tracking at slower rates, the concept of the compartmentalized plasma membrane must be used as the basis. Better yet, high-speed methods should be employed to directly observe the hop diffusion of molecules, because all the membrane molecules undergo hop diffusion anyway, and the guesswork based on the images averaged over a long camera frame time (i.e., blurred images) always leave some ambiguities. In addition, high-speed SPT is not particularly difficult or expensive to introduce in the lab, compared with, for example, confocal or total internal reflection fluorescence microscopy.

Plasma Membrane Compartmentalization is Universally Found Among Mammalian Cells in Culture

The concerns about the credibility of phospholipid hop diffusion, summarized above as well as in Box 4, would be greatly diminished if the plasma membrane compartmentalization were generally found in many types of cultured cells and if its underlying causes were characterized (as described above, hop diffusion could not be detected in liposomes or in blebbed areas of the plasma membrane). Therefore, we asked how universal this plasma membrane compartmentalization may be. Using DOPE, Murase et al. (35; unpublished observations) found such plasma

membrane compartmentalization in all nine mammalian cell types examined thus far. In addition, they found that the compartment size varies greatly, from 30 nm up to 230 nm, and also that the residency time of DOPE ranges between 1 and 17 ms (Figure 2*b*), depending on the cell type. These results disregarded the possibility that the hop-type movement may be induced by the CMOS-type camera employed in these high-speed measurements (Box 4).

THE MEMBRANE-SKELETON FENCE MODEL AND THE ANCHORED-TRANSMEMBRANE PROTEIN PICKETS MODEL

Both Membrane Proteins and Lipids Undergo Hop Diffusion in the Partitioned Plasma Membrane

The key to understanding the underlying mechanism for these two issues, the reduced diffusion rates in the plasma membrane and the suppression of diffusion upon molecular complex formation, was brought about by high-speed single-molecule observations, as described above. However, we have examined only the single-molecule results obtained for lipids thus far in this review. The natural question then is, What is known about transmembrane proteins in the cell membrane?

In fact, the first observation of hop diffusion in the plasma membrane was made with transmembrane proteins: transferrin receptor and $\alpha 2$ -macroglobulin receptor. Using SPT (8–10, 19, 27, 31, 61, 66), Sako & Kusumi (46) directly observed the hop diffusion of membrane molecules: Transferrin receptor and $\alpha 2$ -macroglobulin receptor are temporarily confined within a compartment, and then these molecules hop to an adjacent apposed compartment where they again become trapped temporarily. By repeating such confinement and hop movements between the compartments, the receptor molecules cover macroscopic areas. Because virtually all the examined transferrin receptor and $\alpha 2$ -macroglobulin receptor molecules underwent hop diffusion, it was proposed that the entire plasma membrane is basically partitioned into small compartments with regard to translational diffusion of transmembrane proteins (except for specialized membrane domains, such as clathrin-coated pits, cell-cell and cell-substrate junctions, and microvilli).

Furthermore, all the transmembrane proteins examined thus far, including E-cadherin (48), transferrin receptor (46), $\alpha 2$ -macroglobulin receptor (46), CD44 (K. Ritchie & A. Kusumi, unpublished observations), band 3 (74), stem cell factor receptor (T. Kobayashi, M. Murakami & A. Kusumi, unpublished observations), and a G protein-coupled receptor (K. Suzuki & A. Kusumi, unpublished observations) undergo hop diffusion. The SPT-determined macroscopic diffusion coefficients for these molecules (reflecting the hop-diffusion rate over many compartments) are basically consistent with the single fluorescent molecule video imaging (SFVI) data obtained at slow rates and the traditional FRAP data (Table 1) (T. Fujiwara, K. Iwasawa & A. Kusumi, unpublished observations). However, due

to crosslinking effects, the SPT diffusion coefficients may be smaller by a factor of 1 to 5, depending on the molecules and cells (Box 1). Cross-linking would decrease the hop rate, but would be unlikely to affect the compartment size, and thus the correct residency time within a compartment could be estimated by using the equation (compartment size determined by high-speed SPT)²/(4 × macroscopic diffusion coefficient obtained by SFVI).

The Membrane-Skeleton Fence Model for Temporary Corralling of Transmembrane Proteins

What makes the boundaries between these compartments for transmembrane proteins? On the basis of the single-molecule observation data and the optical trapping results, and by using cells with a modulated cytoskeleton or the modulated cytoplasmic domain of transmembrane proteins (13, 14, 18, 30, 31, 46, 48, 75) (see below and Box 7), the membrane-skeleton fence, or membrane-skeleton corralling, model was proposed (Figure 5, left, see color insert). Transmembrane proteins protrude into the cytoplasm and, in this model, their cytoplasmic domains collide with the membrane skeleton, inducing temporary confinement or corralling of the transmembrane proteins within the membrane-skeleton mesh. The transmembrane proteins then hop to an adjacent compartment. Transmembrane proteins may hop between the compartments when a space that allows the passage of the cytoplasmic domain of the transmembrane protein is formed between the membrane and the membrane skeleton. This space is formed as a result of the thermal fluctuation of these structures, when the actin filament that forms the compartment boundary temporarily dissociates and when the transmembrane protein incidentally has sufficient kinetic energy to overcome the confining potential energy of the compartment barrier when it is in the boundary region. This model was supported by Monte Carlo simulation results (52, 53), as well as by a comparison of the membrane-skeleton structure on the cytoplasmic surface of the plasma membrane observed by atomic force microscopy (71) with a three-dimensional reconstruction using electron microscope-computed tomography (N. Morone, J. Usukura, S. Yuasa & A. Kusumi, unpublished observations). In particular, in the human erythrocyte ghost, the compartment size detected by diffusing band 3 (74) and the mesh size (71) determined by atomic force microscopy were similar to each other, providing additional support.

Before the single-molecule era, a few FRAP reports indicated that the smaller macroscopic diffusion coefficients in the plasma membrane, compared to those found in artificial membranes, may be caused by the membrane skeleton associated with the cytoplasmic surface of the plasma membrane (39, 52, 53, 63, 65, 72, 75, 76, 81). The lateral diffusion coefficients of transmembrane proteins were increased in blebbed membranes or after partial depolymerization of actin filaments (39, 72, 81); however, the results of drug treatments that partially depolymerized actin may be complicated and somewhat unpredictable (35, 39, 46).

Sheetz et al. (65) found that the transmembrane protein band 3 (the majority of the ConA receptor observed in this study is band 3) diffuses approximately 10 times faster in spectrin-deficient mutant mouse erythrocytes than in normal cells. In mammalian red blood cells, the spectrin meshwork, instead of the f-actin network, forms the membrane skeleton. To explain these results, the model of the membrane-skeleton picket fence that reduces the translational diffusion coefficient of transmembrane proteins was first proposed by Sheetz (63). Tsuji and colleagues (75, 76) carried out both translational and rotational diffusion measurements for the transmembrane protein band 3 in human red blood cell ghost membranes, providing the first data substantiating the picket fence model. They found that the band 3 passage across the membrane-skeleton fence is due to the dissociation of the spectrin tetramers into dimers, and that the rotational diffusion of band 3 was unaffected by the dimer-tetramer equilibrium [spectrin tetramer-dimer equilibrium gate model or SPEQ-gate model (75)]. The percolation threshold analysis advanced by Saxton (49, 52, 53) played an important role in interpreting these results. As such, data showing the involvement of the membrane skeleton in the reduction of the translational diffusion rate were abundant even before the era of single-molecule observations, but direct observations of molecules undergoing short-term diffusion within a compartment (made of the membrane skeleton) and long-term hop diffusion over the compartments had to wait until single-molecule technologies became available (16, 30, 31, 46, 74).

The Model of Anchored-Transmembrane Protein Pickets, Which Work for All the Membrane Molecules in the Plasma Membrane

What makes the compartment boundaries work for phospholipids located in the outer leaflet of the membrane (Figures 1 and 3)? Fujiwara et al. (18) and Murase et al. (35) examined the involvement of the membrane skeleton, as well as the effects of the extracellular matrices, the extracellular domains of membrane proteins, and the cholesterol-rich raft domains on phospholipid hop diffusion, by modulating these membrane-associated molecules and structures. Surprisingly, they found that the phospholipid movement was affected only when they modulated the membrane skeleton, consistent with the previous FRAP observation (although the way in which drug treatment actually influences FRAP is complicated; see References 29, 73, 81). The observation that simple-Brownian diffusion of DOPE in membrane blebs (73, 81) (particularly after further treatment with latrunculin) was as fast as that found in giant liposomes (18) (with a diffusion coefficient of approximately $9 \mu\text{m}^2 \text{s}^{-1}$) further supported the involvement of the actin membrane-skeleton in the temporary confinement of DOPE in the membrane compartments. All these results point to the involvement of the membrane skeleton in both the temporary corralling and hop diffusion of phospholipids, and they refute many of the issues raised against the fidelity of SPT results using gold probes, as summarized in Box 4.

How can the movement of DOPE molecules located in the extracellular leaflet of the membrane (DOPE may flip, but the large gold particle cannot get into the cytoplasm) be suppressed by the membrane skeleton, which is located on the cytoplasmic surface of the membrane? DOPE and the membrane skeleton cannot interact directly. To reconcile this apparent contradiction, the anchored-transmembrane protein picket model was proposed (Figure 5, right). In this model, various transmembrane proteins anchored to and lined up along the membrane skeleton (fence) effectively act as rows of pickets (these transmembrane proteins act like posts for the fence, and are thus termed pickets) against the free diffusion of phospholipids, owing to steric hindrance as well as to the hydrodynamic friction-like effects of immobilized anchored-transmembrane protein pickets. The hydrodynamic friction-like effect, first proposed by Hammer's group (5, 6), is particularly strong when exerted by immobile molecules, and it propagates over several nanometers (this effect is prominent in the membrane because the membrane viscosity is much greater than the viscosity of water, by a factor of ≈ 100). Therefore, when these transmembrane proteins are lined up along the membrane skeleton at a density over a certain threshold (a series of Monte Carlo simulations by Fujiwara et al. indicated that 20%–30% coverage of the intercompartmental boundary by these anchored-transmembrane protein pickets is sufficient to reproduce the experimentally observed residency time of 11 ms in a 230-nm compartment in NRK cells), the rows of pickets on the membrane-skeleton fences become effective diffusion barriers that confine the phospholipids for some time. Note that these transmembrane picket proteins do not have to be stably bound to the membrane skeleton for a long time. Assuming that the boundary region between the compartments is 10 nm wide, it takes approximately 10 μ s for a molecule to traverse this region. Therefore, the zeroth approximation is that if a transmembrane protein is bound to the membrane skeleton for at least 10 μ s, then it becomes an effective picket to participate in the formation of the diffusion barrier. Note that in this model the transmembrane proteins anchored to the membrane skeleton are coupling the membrane skeleton, which is located on the cytoplasmic surface of the membrane, to the phospholipids that are located in the outer leaflet of the membrane.

The anchored-transmembrane protein pickets would be operative on any molecules incorporated into the membrane, including transmembrane proteins. Therefore, the diffusion of transmembrane proteins will be doubly suppressed in the membrane. Both the fence and picket will act on transmembrane proteins.

Several reports employing FRAP or low-speed (video rate or slower) single-molecule tracking have noted the absence of an effect of actin depolymerization on the movement of various membrane molecules (18, 35, 60, 79). These treatments tend to increase the compartment size but decrease the hop rate (because the frequency of collisions of membrane molecules with the compartment boundaries decreases owing to the increase in the compartment size) (18, 35), producing opposite effects on the macroscopic diffusion coefficients measured by these techniques and leading to minor increases in the macroscopic diffusion coefficients, by a factor of 1–2, depending on the cell type (18, 35). A clear example is found in Table 5

in Murase et al. (35): After cytochalasin treatment, the average compartment size increased from 45 to 87 nm, but the hop rate for gold-tagged DOPE decreased from an average of once every 15 ms to once every 39 ms, thus only slightly changing the macroscopic diffusion coefficient, from 0.042 to 0.046 $\mu\text{m}^2 \text{s}^{-1}$. After ensemble-averaging over many molecules observed by FRAP, or too much time averaging in low-time-resolution single-molecule tracking (due to a slow frame rate, a long frame time, or both), such small changes in the motional characteristics of the membrane molecules may easily be missed. Furthermore, the use of high concentrations of actin-depolymerizing drugs and/or the long incubation periods often employed in cell biological studies may complicate the results. Thus high-speed single-molecule tracking methods may be the best observation choice. For further details, see the online supplemental material in References 34 and 29.

OLIGOMERIZATION-INDUCED TRAPPING

Diffusion rate reduction or immobilization of membrane molecules upon oligomerization or molecular complex formation may be one of the most physiologically important consequences of plasma membrane compartmentalization by the membrane-skeleton fences and the anchored-transmembrane protein pickets. As stated above, upon oligomerization or molecular complex formation, the macroscopic diffusion coefficients of membrane molecules are decreased greatly (Table 2). The fluid mosaic model and the two-dimensional continuum fluid model (45, 69) cannot explain such large decreases in the macroscopic diffusion coefficients.

The partitioning of the plasma membrane into many small compartments by the membrane-skeleton fences and the anchored-transmembrane protein pickets clearly explains why the diffusion in the plasma membrane is sensitive to the formation of molecular complexes (Figure 6, right, see color insert), in contrast to the prediction from the two-dimensional continuum fluid model (Figure 6, left). Monomers of membrane molecules may hop across the picket fence line with relative ease, but upon molecular complex formation, the complexes as a whole, rather than single molecules, have to hop across the picket fence line all at once; therefore, these complexes likely have a much slower rate of hopping between the compartments. In addition, owing to the avidity effect, molecular complexes are more likely to be bound or tethered to the membrane skeleton, perhaps temporarily, which also induces (temporary) immobilization or trapping of molecular complexes (Figure 6, right). Such enhanced confinement and binding effects induced by oligomerization or molecular complex formation are collectively termed oligomerization-induced trapping (23, 30).

This oligomerization-induced trapping might be critically important in the temporary confinement of a cytoplasmic signal at the early stages of signal transduction. When an extracellular signal is received by a receptor molecule, the receptor often forms oligomers and signaling complexes. Because of the oligomerization-induced trapping, these oligomeric complexes tend to be trapped in the same membrane-skeleton compartment where the extracellular signal was received.

TABLE 2 Compartment sizes determined by high-speed SPT, and the residency times for monomeric DOPE (Cy3-DOPE, SFVI) and oligomeric DOPE (gold-tagged DOPE, SPT) calculated from the macroscopic diffusion coefficients in the time window of 100 ms using the compartment size. See Murase et al. (35) for details

Cell type	Compartment size (L) ^a (nm)	Residency time (τ) ^b (ms)	
		Monomeric DOPE	Oligomeric DOPE
FRSK	41 (46 ± 20)	2.3	9.8
CHO-B1	32 (42 ± 32)	1.0	4.8
HEPA-OVA	36 (40 ± 15)	1.5	5.2
PtK2	43 (44 ± 16)	0.97	1.5
HEK293	68 (71 ± 31)	3.0	8.4
HeLa	68 (68 ± 27)	5.4	14
T24	110 (120 ± 53)	17	16 ^c

^aThe compartment size was directly obtained by SPT, carried out at time resolutions of 25 μ s using Gold-DOPE. $L = (L_x L_y)^{1/2}$. Median values are shown. Mean values and standard deviations are shown in parentheses. The SDs include, in addition to the experimental error, the true variations in the diffusion coefficient or the compartment size for individual particles.

^bFor monomeric DOPE, the residency time was calculated using $D_{100\text{ms}}$ (median), obtained from SFVI observations of Cy3-DOPE, and the compartment size (L , median), obtained from SPT of Gold-DOPE using the equation $\tau = L^2/4D_{100\text{ms}}$. For oligomeric DOPE, the median values obtained from SPT observations of Gold-DOPE were used. $D_{100\text{ms}}$ values for monomeric Cy3-DOPE in FRSK, CHO-B1, HEPA-OVA, PtK2, HEK293, HeLa, and T24 cells were obtained by using SFVI. $D_{100\text{ms}}$ values for oligomeric DOPE were obtained by using SPT of Gold-DOPE probes, which are colloidal gold probes coated with very low amounts of Fab antibodies, inducing low levels of cross-linking while retaining reasonable levels of specific binding.

^cSince the level of oligomerization with these gold probes is low, the cells with larger mesh sizes, T24 and NRK cells with compartment sizes of 110 nm and 230 nm, respectively, exhibit only minor changes in $D_{100\text{ms}}$ upon oligomerization by the gold probes. The oligomerization effect is more apparent when the macroscopic diffusion coefficient is estimated at longer time windows. In T24 cells, $D_{100\text{ms}}$ was found to depend on the level of cell confluency in the culture dish. The values at $\sim 10\%$ confluency (0.17 and 0.19 $\mu\text{m}^2 \text{s}^{-1}$ for monomeric and oligomeric DOPE, respectively) were used to calculate the residency times in this table, because we carry out various experiments with T24 cells at $\sim 10\%$ confluency. At 50 and 70% confluency, the median values for $D_{100\text{ms}}$ are 0.29 and 0.41 $\mu\text{m}^2 \text{s}^{-1}$, respectively. The other cells were observed when they were 30–40% confluent.

Therefore, the membrane-skeleton fence and the anchored-transmembrane protein pickets temporarily help to confine the cytoplasmic signal to the place where the extracellular signal was received. Such spatial confinement is particularly important for signals that induce local or polarized reorganization of the cytoskeleton or chemotactic events.

This would not occur in the absence of membrane-skeleton fences and pickets (Figure 6, left). If there were no such structures, then even when the signaling complex is formed, the diffusion rate of such a complex would be almost identical to that of the single-receptor molecules, as the diffusion theory teaches us (45).

Therefore, in the plasma membrane, oligomerization or molecular complex formation is tied to immobilization because of the presence of the membrane-skeleton fence and the anchored-transmembrane protein pickets. We have to fully appreciate that the insensitivity of translational diffusion measurements to molecular complex formation, which in fact sounds somewhat paradoxical in the beginning, is true only in reconstituted membranes without the membrane skeleton, and in the cell membrane, the diffusion coefficient is a sensitive parameter to detect molecular complex formation.

A PARADIGM SHIFT OF THE LONG-RANGE STRUCTURE OF THE CELL MEMBRANE

A Paradigm Shift from the Two-Dimensional Continuum Fluid to the Compartmentalized Fluid

As described above, the membrane-skeleton fence and the anchored-transmembrane protein pickets together solved the two long-standing problems of molecular diffusion in the plasma membrane: (a) the oligomerization-induced temporary trapping and (b) the reduced diffusion coefficients of membrane molecules in the plasma membrane, which are smaller than those found in artificial membranes by factors of 5 to 50.

A paradigm shift for the concept of the plasma membrane structure in space scales larger than 10 nm may be required, from the two-dimensional continuum fluid to the compartmentalized fluid, in which its constituent molecules undergo hop diffusion over the compartments. The cell appears to have developed (during evolution) means to control the long-range diffusion of membrane molecules and to make it sensitive to the diffusant size. The long-range control of diffusion appears to be carried out by the actin-based membrane skeleton and its associated transmembrane-protein pickets through their partitioning (corralling) and tethering effects, which are enhanced upon molecular complex formation by diffusing membrane molecules.

Other Related Observations and Models Regarding the Reduction of Diffusion Coefficients in the Plasma Membrane Compared to Those in Artificial/Reconstituted Membranes

Good reviews for somewhat older literature were published in this series of Annual Reviews by Sheetz (64) and Saxton & Jacobson (59). Here, we categorize the various previous observations into the following three groups.

INVOLVEMENT OF THE MEMBRANE SKELETON The barrier effects of the membrane skeleton have been proposed by Sheetz et al. (65), Sheetz (63), and Edidin et al. (13). The barrier-free path found in the last paper is much greater than the compartment size determined subsequently by SPT (18, 35, 46, 48) and optical

trapping (47, 48), 3.5 μm versus 36 nm in the case of HEPA-OVA cells (35), but this is probably due to the large force employed in their earlier research. The dragged molecule probably deformed the membrane skeleton until it was released from the optical trap owing to the force exerted by the deformed membrane skeleton. The effects of these corrals, particularly their percolation effects, have been investigated by Saxton (52, 53). In related research, the effect of transient binding was studied experimentally by Suzuki & Sheetz (70) and by Saxton (57), who used Monte Carlo simulations.

PROTEIN CROWDING MODEL This concept was advanced by Sheetz (64), with a special emphasis on the large extracellular domains of many glycoproteins. The effect of their large glycochains was investigated by Lee et al. (33), who showed that they exert a moderate effect on the diffusion coefficient. Furthermore, the long-range interactions of glycoproteins have been proposed by Abney & Scalettar (1). However, Peters & Cherry (41) found that the diffusion coefficients for proteins and lipids are only moderately affected by the protein-to-lipid ratio: The coefficients decrease by approximately a factor of two with an increase in the protein-to-lipid ratio by approximately a factor of two, in the range in which the protein (bacteriorhodopsin) may still behave as monomers (3). This is consistent with the Monte Carlo simulation results, in which the influence of simple protein crowding in the membrane on the diffusion was moderate as long as the diffusion obstacles are mobile (49, 50). The crowding effect might appear as increased viscosity in the extracellular and intracellular surfaces of the cell membrane or within the cell membrane, in an independent way (24, 33, 82). However, Fujiwara et al. (18) and Murase et al. (35) showed that the diffusion coefficient within a compartment is comparable to that found in liposomes, and Tank et al. (73) found dramatically increased macroscopic diffusion coefficients in membrane blebs for both membrane proteins and lipids. Therefore, the crowding effects modulate the diffusion coefficient to a limited extent.

Two considerations may be critically important when protein crowding in the membrane is considered. (a) Does the crowding involve the proteins that are anchored to the membrane skeleton (immobile proteins) or does crowding induce the binding of some of the proteins (perhaps due to the avidity effect of protein complexes) to the membrane skeleton, and thereby cause their immobilization? (b) Does the crowding induce clusters of some of the proteins (even though their lifetimes may be very short)?

First, as suggested above, it is critically important to differentiate the effects of immobile molecules from those of mobile molecules. As shown by Saxton (49, 50), molecules become true diffusion obstacles only when they are immobilized. Therefore, crowding becomes important only when some of the crowded molecules are immobilized. In fact, this is likely the case with the transmembrane protein pickets; they are immobilized on the membrane skeleton and thereby act as diffusion barriers. In addition, their alignment on the membrane skeleton is important to form pickets in a row to create an effective boundary; also note again

that even if their bound time is limited to only 10 μ s, during this period they act as anchored pickets, i.e., effective diffusion barriers. To think of diffusion obstacles without critically examining their levels of immobilization does not appear to be correct or productive.

Second, simple crowding should not be confused with the induction of oligomerization upon increase in protein concentration. When protein concentrations are raised, oligomers tend to form, although they may be transient, with lifetimes on the order of microseconds to milliseconds (28). If this occurs, their diffusion coefficients drop dramatically owing to the enhanced effects of corralling and binding by the membrane skeleton. Furthermore, when the oligomers or the molecular complexes become anchored to the membrane skeleton (because of the avidity effect), they become diffusion obstacles to other membrane molecules. Large extracellular domains of membrane-associated molecules may affect the diffusion rate, as proposed by Sheetz (64), but this may occur not because of the simple crowding effect of extracellular domains, but because they induce oligomerization. Hemagglutinin molecules are expressed as trimers on the cell surface in their natural transmembrane form as well as in an artificial GPI-anchored form owing to the presence of the trimer formation sites in the extracellular domain. The diffusion coefficients of both types of molecules were substantially smaller than those for most transmembrane proteins (26, 67), consistent with oligomerization-induced trapping [perhaps amplified because of the formation of stable rafts (67)] rather than simple crowding.

MODULATING EFFECTS OF CHOLESTEROL The effects of the partial removal of cholesterol are complicated. If the major function of cholesterol is to form the lipid raft domains, then its influence may be somewhat limited because (assuming the diffusion characteristics in the raft domain are similar to those in the liquid-ordered domain in artificial membranes) the diffusion coefficient within the liquid-ordered domain is smaller by only a factor of 2, and membrane molecules appear to cross the boundaries between the raft domain and the bulk domain freely (11, 12). However, Kwik et al. (32) found that this treatment could induce actin reorganization, causing large reductions in both the macroscopic diffusion coefficient and the distance that an MHC class I molecule could be dragged. If this occurs, even after cholesterol is replenished, it will take hours to recover the original diffusion coefficient. Therefore, a good test to examine whether this happens may be to replenish cholesterol and see if the diffusion coefficient reaches the level found before the cholesterol removal within an hour or so.

Summary of the Evidence Supporting the Membrane-Skeleton Fence and Anchored-Transmembrane Protein Picket Models for Compartmentalization of the Cell Membrane

Here, the observations that support the models of membrane-skeleton fence and anchored-transmembrane protein pickets are summarized. Any membrane model

must be compatible with these observations. So far, we have not found any other models that could be consistent with all of these observations: Some models could explain one or several of these observations, but not *all* of these observations.

It is neither wise nor productive to ponder interminably over the results obtained by just a single method, i.e., the kinetic (not even mechanic) observations of molecules, following trajectories. Furthermore, thus far the only means by which to implement quantitative analysis of diffusion in the cell membrane has been to use the plots based on the relationship between the MSD and the time interval (similar to those shown in Figures 2 and 4), but much information is lost during the process of producing these plots from the trajectory. Therefore, in addition to using single-molecule tracking data, we emphasize that other lines of evidence must be considered when models or hypotheses are created.

Because of space limitations, we only briefly state the experimental results. Detailed explanations, their relations to various models, and original literature are given in Box 7.

1. Oligomerization of transmembrane proteins or lipids reduces the macroscopic diffusion coefficient and the intercompartmental hop rate without affecting the compartment size [oligomerization-induced trapping (23, 35)].
2. The compartment sizes detected by transmembrane proteins (transferrin receptor, α_2 -macroglobulin receptor) and the phospholipid DOPE are the same in all the cell types examined thus far.
3. The compartment size detected by the distance of transmembrane proteins being dragged in optical trap experiments employing weak trapping forces agrees with the compartment size determined by single-molecule diffusion measurements.
4. The optical trapping experiments revealed that the compartment boundaries are elastic.
5. By dragging the membrane skeleton along the plasma membrane, even transmembrane protein molecules that are not bound to the membrane skeleton could be laterally translocated.
6. The compartment sizes detected from diffusion measurements of transmembrane proteins and lipids are consistent with the mesh size of the membrane skeleton on the cytoplasmic surface of the plasma membrane, as determined by atomic force microscopy or electron microscope-computed tomography.
7. Monte Carlo simulations reproduced the experimentally observed residency times when only 20%–30% of the compartment boundaries were occupied by the anchored-transmembrane protein pickets. This represents the anchoring of approximately 15% of the total transmembrane proteins in the plasma membrane.
8. Hop diffusion of transmembrane proteins and lipids (determined by statistical analyses) depends on the integrity of the membrane skeleton. Hop

diffusion cannot be found in liposomes or membrane blebs. In these membranes, the membrane molecules undergo rapid, simple Brownian diffusion that can be characterized by a single diffusion coefficient of $5\text{--}10\ \mu\text{m}^2\ \text{s}^{-1}$ for DOPE or $3\ \mu\text{m}^2\ \text{s}^{-1}$ for transmembrane proteins.

9. Mild treatments with jasplakinolide, which stabilizes the actin filaments, reduces the macroscopic diffusion coefficient, without strongly affecting the compartment size, by decreasing the hop frequency.
10. The instances of hops in single-molecule trajectories are detectable with a computer program in the analysis of single-molecule observations with sufficient time resolution.
11. The hop rate of transmembrane proteins increases after the partial removal of the cytoplasmic domain of transmembrane proteins.
12. The hop diffusion is not affected by the removal of the major fraction of the extracellular domains of transmembrane proteins and the extracellular matrix.
13. The removal of cholesterol has no major effects on hop diffusion.
14. In hippocampal neurons, the macroscopic diffusion coefficient of DOPE in various regions and developmental stages of the cells correlates well with the concentration of the membrane skeletal proteins, such as ankyrin and actin (see below). Furthermore, the level of reduction is nonlinearly related to the ankyrin concentration in the initial segment membrane. At the initial stages of ankyrin assembly, the lipid diffusion is hardly affected, but when it reaches a certain threshold level, the DOPE diffusion coefficient suddenly decreases by several hundred-fold.

DEVELOPMENTAL FORMATION OF A DIFFUSION BARRIER IN THE NEURONAL INITIAL SEGMENT CELL MEMBRANE

The neuron has two distinct domains: the somatodendritic domain, which functions in the input of the electrical signal, and the axonal domain, which is responsible for the output of the signal. Each domain has its characteristic membrane proteins. However, the plasma membrane is one continuous membrane; therefore, there must be a diffusion barrier in the boundary region between the two domains so that the cell can prevent the intermixing of the membrane molecules located in each of these two domains. The membrane area that is located between these two main domains and separates these two domains is called the initial segment (IS), an elongated domain with a length of $\approx 30\ \mu\text{m}$ in mature neurons, located at the foot of the axon. Nakada et al. (37) found that neuronal cells develop diffusion barriers in the plasma membrane by using the membrane skeleton fences and the anchored-transmembrane protein pickets (37). In fact, one major function of these fences and pickets may be to form large diffusion barriers in the cell membrane. Owing to page limitations, these studies are summarized in Box 8.

CONCLUSIONS

Any observation requires time resolutions comparable to or shorter than the time period characteristic of observed events. This fundamental principle does not seem to have been fully appreciated in the membrane biophysics community. Abundant evidence exists that indicates that the plasma membrane is a nonideal mixture of molecules with various levels of miscibilities and in addition contains immobile molecules that may be bound to the underlying cytoskeleton, suggesting the presence of domains and molecular complexes with different sizes and lifetimes. However, given the large body of literature that contains simple-minded applications of Brownian diffusion to the plasma membrane, as well as the fractal character of the basic type of Brownian diffusion (self-similar trajectories are obtained even when the observation frequency, i.e., the shutter repetition frequency of the camera, is changed, and because the movement is characterized by a single parameter, the diffusion coefficient, the same diffusion coefficient can be obtained irrespective of the observation frequency), researchers have been slow to adopt the high-frequency observation methods.

In plasma membrane research, researchers need to realize that the time resolution (frame exposure time or frame repetition time, depending on the situation) is coupled to the examined space scales by way of diffusion. A molecule with a microscopic diffusion coefficient of $9 \mu\text{m}^2 \text{s}^{-1}$ can cover areas with a radius of 60 nm to $1.8 \mu\text{m}$ (Gaussian half width) within time windows of 100 μs to 100 ms. This clearly exemplifies the fact that observations of molecular events occurring in the subdomains in the plasma membrane, whether one has a sufficiently high observation frequency (sufficiently short time window), should be considered seriously in the design and interpretation of the experiments.

From the argument above, it is also apparent that membrane researchers always have to deal with nonhomogeneous systems. To find out how a molecular species of interest behaves in such an inhomogeneous system, researchers must seriously reconsider the employment of conventional scientific measurements, which were basically developed for observations under or close to homogeneous conditions in a test tube. These methods are often said to involve "ensemble averaging"; however, in the case of the plasma membrane, we have not determined what kind of ensemble the membrane has, and thus "ensemble averaging" is an undefined word for the investigations of the plasma membrane at the present stage. To understand the molecular events occurring in a system with high levels of inhomogeneities, researchers could track the behavior of single molecules and, by repeating the observations for many molecules, the nature of the inhomogeneity in behavior (like interactions with various molecules), in space, and in time could be investigated.

However, to achieve such examinations, as emphasized at the beginning of this section, the time resolution of the single-molecule method employed must be considered. To understand what a molecule does, and when and where it does that, the single-molecule method employed must have a sufficient time resolution (but note that, at the same time, the length of the trajectory must be kept sufficiently long). Furthermore, researchers must understand the limitations of the employed

methods in terms of both time and space scales. (As described above, this space scale is not simply the intrinsic spatial resolution of the method; it is also limited by the time resolution that is coupled to the space scales via the diffusion coefficient.) In fact, it seems to us that one major source of great confusion in raft research is due to the lack of appreciation for these spatiotemporal limitations of the technologies employed by raft researchers and to the consequent overinterpretations, or misinterpretations, of the measurements.

On the basis of these arguments, we envisage that high-speed single-molecule tracking will become an important tool for studying the molecular events occurring in the plasma membrane in living cells. We hope that many readers of this review will become interested in high-speed single-molecule tracking and will adopt this new approach in their own studies.

In this review, we somewhat emphasized the use of SPT for high-speed single-molecule tracking. However, the development of new cameras with higher sensitivities and dynamic ranges, as well as new fluorescent dyes or proteins with higher extinction coefficients, quantum yields, and photostability, will make single fluorescent molecule tracking at reasonably high rates with decent signal-to-noise ratios and reasonably long tracking times more accessible. For both participants and observers, this will be a promising field in plasma membrane research in the near future.

ACKNOWLEDGMENTS

We thank all members of the Kusumi laboratory for their help and discussions in the research described in this review.

The *Annual Review of Biophysics and Biomolecular Structure* is online at <http://biophys.annualreviews.org>

LITERATURE CITED

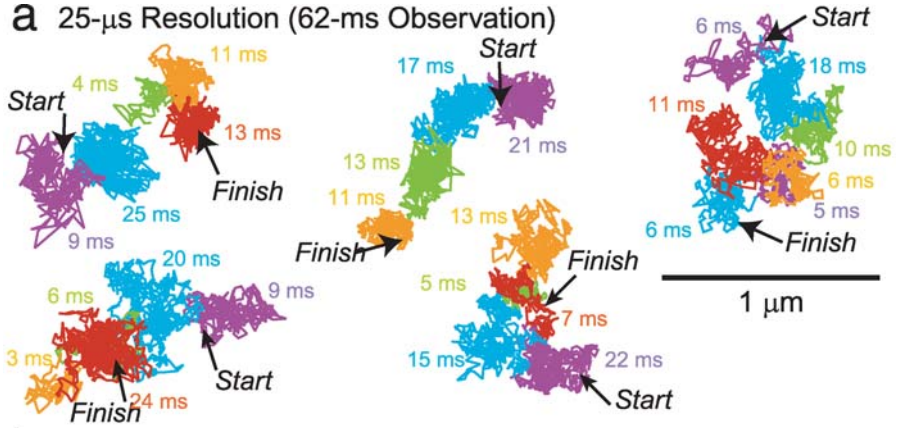
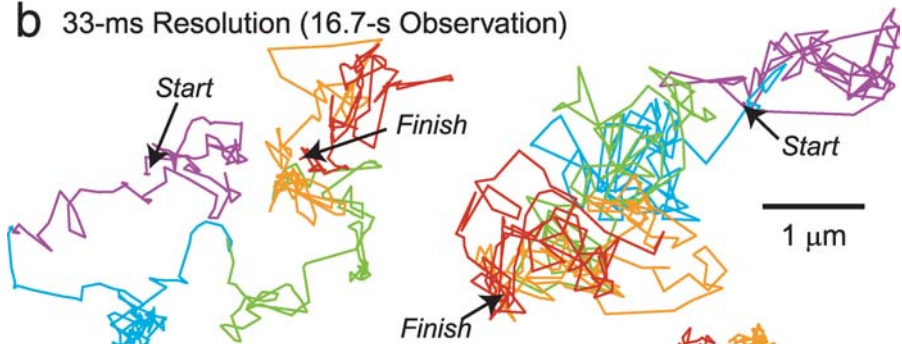
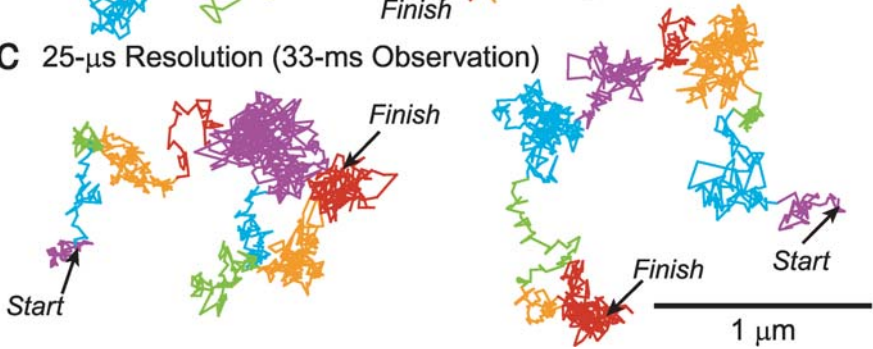
1. Abney JR, Scalettar BA. 1995. Fluctuations and membrane heterogeneity. *Bioophys. Chem.* 57:27–36
2. Ahlen K, Ring P, Tomasini-Johansson B, Holmqvist K, Magnusson KE, Rubin K. 2004. Platelet-derived growth factor-BB modulates membrane mobility of beta1 integrins. *Biochem. Biophys. Res. Commun.* 314:89–96
3. Ashikawa I, Yin JJ, Subczynski WK, Kouyama T, Hyde JS, Kusumi A. 1994. Molecular organization and dynamics in bacteriorhodopsin-rich reconstituted membranes: discrimination of lipid environments by the oxygen transport parameter using a pulse ESR spin-labeling technique. *Biochemistry* 33:4947–52
4. Axelrod D, Ravdin P, Koppel DE, Schlessinger J, Webb WW, et al. 1976. Lateral motion of fluorescently labeled acetylcholine receptors in membranes of developing muscle fibers. *Proc. Natl. Acad. Sci. USA* 73:4594–98
5. Bussell SJ, Hammer DA, Koch DL. 1994. The effect of hydrodynamic interactions on the tracer and gradient diffusion of integral membrane-proteins in lipid bilayers. *J. Fluid Mech.* 258:167–90

6. Bussell SJ, Koch DL, Hammer DA. 1995. Effect of hydrodynamic interactions on the diffusion of integral membrane proteins: diffusion in plasma membranes. *Biophys. J.* 68:1836–49
7. Chang CH, Takeuchi H, Ito T, Machida K, Ohnishi S. 1981. Lateral mobility of erythrocyte membrane proteins studied by the fluorescence photobleaching recovery technique. *J. Biochem.* 90:997–1004
8. De Brabander M, Geuens G, Nuydens R, Moeremans M, De Mey J. 1985. Probing microtubule-dependent intracellular motility with nanometre particle video ultramicroscopy (nanovid ultramicroscopy). *Cytobios* 43:273–83
9. De Brabander M, Nuydens R, Geerts H, Hopkins CR. 1988. Dynamic behavior of the transferrin receptor followed in living epidermoid carcinoma (A431) cells with nanovid microscopy. *Cell Motil. Cytoskelet.* 9:30–47
10. De Brabander M, Nuydens R, Ishihara A, Holifield B, Jacobson K, Geerts H. 1991. Lateral diffusion and retrograde movements of individual cell surface components on single motile cells observed with nanovid microscopy. *J. Cell. Biol.* 112:111–24
11. Dietrich C, Bagatolli LA, Volovyk ZN, Thompson NL, Levi M, et al. 2001. Lipid rafts reconstituted in model membranes. *Biophys. J.* 80:1417–28
12. Dietrich C, Volovyk ZN, Levi M, Thompson NL, Jacobson K. 2001. Partitioning of Thy-1, GM1, and cross-linked phospholipid analogs into lipid rafts reconstituted in supported model membrane monolayers. *Proc. Natl. Acad. Sci. USA* 98:10642–47
13. Edidin M, Kuo SC, Sheetz MP. 1991. Lateral movements of membrane glycoproteins restricted by dynamic cytoplasmic barriers. *Science* 254:1379–82
14. Edidin M, Zuniga MC, Sheetz MP. 1994. Truncation mutants define and locate cytoplasmic barriers to lateral mobility of membrane glycoproteins. *Proc. Natl. Acad. Sci. USA* 91:3378–82
15. Erb EM, Tangemann K, Bohrmann B, Muller B, Engel J. 1997. Integrin alphaIIb beta3 reconstituted into lipid bilayers is nonclustered in its activated state but clusters after fibrinogen binding. *Biochemistry* 36:7395–402
16. Fache MP, Moussif A, Fernandes F, Giraud P, Garrido JJ, Dargent B. 2004. Endocytotic elimination and domain-selective tethering constitute a potential mechanism of protein segregation at the axonal initial segment. *J. Cell Biol.* 166:571–78
17. Feder TJ, Brust-Mascher I, Slattery JP, Baird B, Webb WW. 1996. Constrained diffusion or immobile fraction on cell surfaces: a new interpretation. *Biophys. J.* 70:2767–73
18. Fujiwara T, Ritchie K, Murakoshi H, Jacobson K, Kusumi A. 2002. Phospholipids undergo hop diffusion in compartmentalized cell membrane. *J. Cell. Biol.* 157:1071–81
19. Gelles J, Schnapp BJ, Sheetz MP. 1988. Tracking kinesin-driven movements with nanometre-scale precision. *Nature* 331:450–53
20. Golan DE, Brown CS, Cianci CM, Furlong ST, Caulfield JP. 1986. Schistosomula of *Schistosoma mansoni* use lysophosphatidylcholine to lyse adherent human red blood cells and immobilize red cell membrane components. *J. Cell Biol.* 103:819–28
21. Golan DE, Veatch W. 1980. Lateral mobility of band 3 in the human erythrocyte membrane studied by fluorescence photobleaching recovery: evidence for control by cytoskeletal interactions. *Proc. Natl. Acad. Sci. USA* 77:2537–41
22. Hegener O, Prenner L, Runkel F, Baader SL, Kappler J, Haberland H. 2004. Dynamics of beta2-adrenergic receptor-ligand complexes on living cells. *Biochemistry* 43:6190–99
23. Iino R, Koyama I, Kusumi A. 2001. Single molecule imaging of green fluorescent

- proteins in living cells: E-cadherin forms oligomers on the free cell surface. *Biophys. J.* 80:2667–77
24. Jacobson KA, Moore SE, Yang B, Doherty P, Gordon GW, Walsh FS. 1997. Cellular determinants of the lateral mobility of neural cell adhesion molecules. *Biochim. Biophys. Acta* 1330:138–44
 25. Kapitza HG, Ruppel DA, Galla HJ, Sackmann E. 1984. Lateral diffusion of lipids and glycophorin in solid phosphatidylcholine bilayers. The role of structural defects. *Biophys. J.* 45:577–87
 26. Kenworthy AK, Nichols BJ, Remmert CL, Hendrix GM, Kumar M, et al. 2004. Dynamics of putative raft-associated proteins at the cell surface. *J. Cell Biol.* 165:735–46
 27. Kucik DF, Elson EL, Sheetz MP. 1989. Forward transport of glycoproteins on leading lamellipodia in locomoting cells. *Nature* 340:315–17
 28. Kusumi A, Hyde JS. 1982. Spin-label saturation-transfer electron spin resonance detection of transient association of rhodopsin in reconstituted membranes. *Biochemistry* 21:5978–83
 29. Kusumi A, Murakoshi H, Murase K, Fujiwara T. 2005. Single-molecule imaging of diffusion, recruitment, and activation of signaling molecules in living cells. In *Biophysical Aspects of Transmembrane Signaling*, ed. S Damjanovich. Heidelberg: Springer-Verlag. In press
 30. Kusumi A, Sako Y. 1996. Cell surface organization by the membrane skeleton. *Curr. Opin. Cell Biol.* 8:566–74
 31. Kusumi A, Sako Y, Yamamoto M. 1993. Confined lateral diffusion of membrane receptors as studied by single particle tracking (nanovid microscopy). Effects of calcium-induced differentiation in cultured epithelial cells. *Biophys. J.* 65:2021–40
 32. Kwik J, Boyle S, Fooksman D, Margolis L, Sheetz MP, Edidin M. 2003. Membrane cholesterol, lateral mobility, and the phosphatidylinositol 4,5-bisphosphate-dependent organization of cell actin. *Proc. Natl. Acad. Sci. USA* 100:13964–69
 33. Lee GM, Zhang F, Ishihara A, McNeil CL, Jacobson KA. 1993. Unconfined lateral diffusion and an estimate of pericellular matrix viscosity revealed by measuring the mobility of gold-tagged lipids. *J. Cell. Biol.* 120:25–35
 34. Murakoshi H, Iino R, Kobayashi T, Fujiwara T, Ohshima C, et al. 2004. Single-molecule imaging analysis of Ras activation in living cells. *Proc. Natl. Acad. Sci. USA* 101:7317–22
 35. Murase K, Fujiwara T, Umemura Y, Suzuki K, Iino R, et al. 2004. Ultrafine membrane compartments for molecular diffusion as revealed by single molecule techniques. *Biophys. J.* 86:4075–93
 36. Nagle JF. 1992. Long tail kinetics in biophysics? *Biophys. J.* 63:366–70
 37. Nakada C, Ritchie K, Oba Y, Nakamura M, Hotta Y, et al. 2003. Accumulation of anchored proteins forms membrane diffusion barriers during neuronal polarization. *Nat. Cell Biol.* 5:626–32
 38. Nelson S, Horvat RD, Malvey J, Roess DA, Barisas BG, Clay CM. 1999. Characterization of an intrinsically fluorescent gonadotropin-releasing hormone receptor and effects of ligand binding on receptor lateral diffusion. *Endocrinology* 140:950–57
 39. Paller MS. 1994. Lateral mobility of Na,K-ATPase and membrane lipids in renal cells. Importance of cytoskeletal integrity. *J. Membr. Biol.* 142:127–35
 40. Pasenkiewicz-Gierula M, Subczynski WK, Kusumi A. 1991. Influence of phospholipid unsaturation on the cholesterol distribution in membranes. *Biochimie* 73:1311–16
 41. Peters R, Cherry RJ. 1982. Lateral and rotational diffusion of bacteriorhodopsin in lipid bilayers: experimental test of the Saffman-Delbrück equations. *Proc. Natl. Acad. Sci. USA* 79:4317–21
 42. Powles GJ, Mallett MJD, Rickayzen G,

- Evans WAB. 1992. Exact analytic solutions for diffusion impeded by an infinite array of partially permeable barriers. *Proc. R. Soc. London A* 436:391–403
43. Qian H, Sheetz MP, Elson EL. 1991. Single particle tracking. Analysis of diffusion and flow in two-dimensional systems. *Biophys. J.* 60:910–21
44. Roess DA, Horvat RD, Munnelly H, Barisas BG. 2000. Luteinizing hormone receptors are self-associated in the plasma membrane. *Endocrinology* 141:4518–23
45. Saffman PG, Delbrück M. 1975. Brownian motion in biological membranes. *Proc. Natl. Acad. Sci. USA* 72:3111–13
46. Sako Y, Kusumi A. 1994. Compartmentalized structure of the plasma membrane for receptor movements as revealed by a nanometer-level motion analysis. *J. Cell. Biol.* 125:1251–64
47. Sako Y, Kusumi A. 1995. Barriers for lateral diffusion of transferrin receptor in the plasma membrane as characterized by receptor dragging by laser tweezers: fence versus tether. *J. Cell. Biol.* 129:1559–74
48. Sako Y, Nagafuchi A, Tsukita S, Takeichi M, Kusumi A. 1998. Cytoplasmic regulation of the movement of E-cadherin on the free cell surface as studied by optical tweezers and single particle tracking: corralling and tethering by the membrane skeleton. *J. Cell. Biol.* 140:1227–40
49. Saxton MJ. 1982. Lateral diffusion in an archipelago. Effects of impermeable patches on diffusion in a cell membrane. *Biophys. J.* 39:165–73
50. Saxton MJ. 1987. Lateral diffusion in an archipelago. The effect of mobile obstacles. *Biophys. J.* 52:989–97
51. Saxton MJ. 1989. Lateral diffusion in an archipelago. Distance dependence of the diffusion coefficient. *Biophys. J.* 56:615–22
52. Saxton MJ. 1989. The spectrin network as a barrier to lateral diffusion in erythrocytes. A percolation analysis. *Biophys. J.* 55:21–28
53. Saxton MJ. 1990. The membrane skeleton of erythrocytes. A percolation model. *Biophys. J.* 57:1167–77
54. Saxton MJ. 1994. Anomalous diffusion due to obstacles: a Monte Carlo study. *Biophys. J.* 66:394–401
55. Saxton MJ. 1994. Single-particle tracking: models of directed transport. *Biophys. J.* 67:2110–19
56. Saxton MJ. 1995. Single-particle tracking: effects of corrals. *Biophys. J.* 69:389–98
57. Saxton MJ. 1996. Anomalous diffusion due to binding: a Monte Carlo study. *Biophys. J.* 70:1250–62
58. Saxton MJ. 2001. Anomalous subdiffusion in fluorescence photobleaching recovery: a Monte Carlo study. *Biophys. J.* 81:2226–40
59. Saxton MJ, Jacobson K. 1997. Single-particle tracking: applications to membrane dynamics. *Annu. Rev. Biophys. Biomol. Struct.* 26:373–99
60. Schmidt K, Nichols BJ. 2004. A barrier to lateral diffusion in the cleavage furrow of dividing mammalian cells. *Curr. Biol.* 14:1002–6
61. Schnapp BJ, Gelles J, Sheetz MP. 1988. Nanometer-scale measurements using video light microscopy. *Cell Motil. Cytoskelet.* 10:47–53
62. Sheets ED, Lee GM, Simson R, Jacobson K. 1997. Transient confinement of a glycosylphosphatidylinositol-anchored protein in the plasma membrane. *Biochemistry* 36:12449–58
63. Sheetz MP. 1983. Membrane skeletal dynamics—role in modulation of red-cell deformability, mobility of transmembrane proteins, and shape. *Semin. Hematol.* 20:175–88
64. Sheetz MP. 1993. Glycoprotein motility and dynamic domains in fluid plasma membranes. *Annu. Rev. Biophys. Biomol. Struct.* 22:417–31
65. Sheetz MP, Schindler M, Koppel DE. 1980. Lateral mobility of integral membrane proteins is increased in spherocytic erythrocytes. *Nature* 285:510–11

66. Sheetz MP, Turney S, Qian H, Elson EL. 1989. Nanometre-level analysis demonstrates that lipid flow does not drive membrane glycoprotein movements. *Nature* 340:284–88
67. Shvartsman DE, Kotler M, Tall RD, Roth MG, Henis YI. 2003. Differently anchored influenza hemagglutinin mutants display distinct interaction dynamics with mutual rafts. *J. Cell Biol.* 163:879–88
68. Simson R, Yang B, Moore SE, Doherty P, Walsh FS, Jacobson KA. 1998. Structural mosaicism on the submicron scale in the plasma membrane. *Biophys. J.* 74:297–308
69. Singer SJ, Nicolson GL. 1972. The fluid mosaic model of the structure of cell membranes. *Science* 175:720–31
70. Suzuki K, Sheetz MP. 2001. Binding of cross-linked glycosylphosphatidylinositol-anchored proteins to discrete actin-associated sites and cholesterol-dependent domains. *Biophys. J.* 81:2181–89
71. Takeuchi M, Miyamoto H, Sako Y, Komizu H, Kusumi A. 1998. Structure of the erythrocyte membrane skeleton as observed by atomic force microscopy. *Biophys. J.* 74:2171–83
72. Tank DW, Wu ES, Meers PR, Webb WW. 1982. Lateral diffusion of gramicidin C in phospholipid multibilayers. Effects of cholesterol and high gramicidin concentration. *Biophys. J.* 40:129–35
73. Tank DW, Wu ES, Webb WW. 1982. Enhanced molecular diffusibility in muscle membrane blebs: release of lateral constraints. *J. Cell Biol.* 92:207–12
74. Tomishige M, Sako Y, Kusumi A. 1998. Regulation mechanism of the lateral diffusion of band 3 in erythrocyte membranes by the membrane skeleton. *J. Cell Biol.* 142:989–1000
75. Tsuji A, Kawasaki K, Ohnishi S, Merkle H, Kusumi A. 1988. Regulation of band 3 mobilities in erythrocyte ghost membranes by protein association and cytoskeletal meshwork. *Biochemistry* 27:7447–52
76. Tsuji A, Ohnishi S. 1986. Restriction of the lateral motion of band 3 in the erythrocyte membrane by the cytoskeletal network: dependence on spectrin association state. *Biochemistry* 25:6133–39
77. Vaz WL, Criado M, Madeira VM, Schoellmann G, Jovin TM. 1982. Size dependence of the translational diffusion of large integral membrane proteins in liquid-crystalline phase lipid bilayers. A study using fluorescence recovery after photobleaching. *Biochemistry* 21:5608–12
78. Vaz WL, Kapitza HG, Stumpel J, Sackmann E, Jovin TM. 1981. Translational mobility of glycoporphin in bilayer membranes of dimyristoylphosphatidylcholine. *Biochemistry* 20:1392–96
79. Vrljic M, Nishimura SY, Brasselet S, Moerner WE, McConnell HM. 2002. Translational diffusion of individual class II MHC membrane proteins in cells. *Biophys. J.* 83:2681–92
80. Warren GB, Houslay MD, Metcalfe JC, Birdsall NJ. 1975. Cholesterol is excluded from the phospholipid annulus surrounding an active calcium transport protein. *Nature* 255:684–87
81. Wu ES, Tank DW, Webb WW. 1982. Unconstrained lateral diffusion of concanavalin A receptors on bulbous lymphocytes. *Proc. Natl. Acad. Sci. USA* 79:4962–66
82. Zhang F, Crise B, Su B, Hou Y, Rose JK, et al. 1991. Lateral diffusion of membrane-spanning and glycosylphosphatidylinositol-linked proteins: toward establishing rules governing the lateral mobility of membrane proteins. *J. Cell Biol.* 115:75–84

a 25- μs Resolution (62-ms Observation)**b** 33-ms Resolution (16.7-s Observation)**c** 25- μs Resolution (33-ms Observation)

See legend on next page

Figure 1 Representative trajectories of colloidal-gold-tagged DOPE molecules in the plasma membrane of normal rat kidney epithelial (NRK) cells (*a*, *b*) and in the liposomal membrane (*c*) recorded at time resolutions of 25 μ s (*a*, *c*) and 33 ms (*b*). (*a*) The different colors of the trajectories (25- μ s resolution, full length of 62 ms or 2500 points) represent various plausible compartments in the plasma membrane, detected by computer software developed in our laboratory (in a time sequence of purple, blue, green, orange, and red for both time resolutions). (*b*) Although these trajectories (33-ms resolution, full length of 16.7 s or 500 points) were obtained in the cell membrane, they were classified into the simple Brownian mode by our statistical analysis, owing to the lack of sufficient time resolution (33 ms). Different colors are used to simply represent the passage of time (3.3 s for each color). These results show that the simple Brownian nature of diffusion observed at slower rates may be superficially induced by the lack of sufficient time resolution: The confined + hop movement of each DOPE molecule is totally smeared out in video-rate observations. To resolve the hop movement, the camera's frame time must be considerably shorter than the average residency time within a compartment. (*c*) Representative trajectories obtained in the liposomal membrane in the liquid crystalline (l_{α}) phase are shown (25- μ s resolution, full length of 33 ms or 1320 points). Almost all of the trajectories monitored in the liposomal membrane were classified into the simple Brownian diffusion mode, even at a 25- μ s resolution. To warn readers against making superficial judgments, fake (deceiving) compartments are shown in different colors. Typical simple Brownian trajectories, such as these shown here, always contain regions where the molecules appear to be staying longer than statistically expected from the average diffusion coefficient, and therefore, one must always use statistical analysis to make useful statements based on these measurements. However, even with the naked eye, after being educated by the outputs of the computer program that statistically detects diffusion anomaly in the observed trajectories, the difference between the trajectories shown in (*a*) and (*c*) is often clear. In hop trajectories, the adjacent compartments are closely apposed to each other, generally exhibiting a pattern composed of apposed patches, whereas in simple Brownian trajectories, the apparently dense areas tend to be connected by trajectories that look like loose strings. In addition, the detected compartment in (*a*) is more densely populated with points than the fake compartments in (*c*).

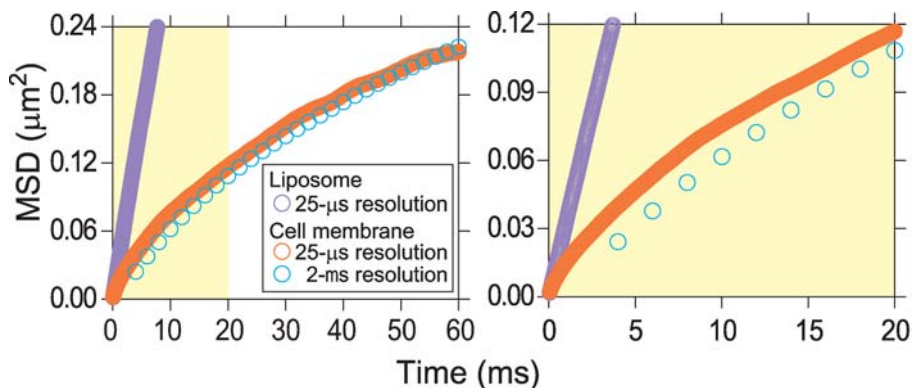


Figure 2 The mean-square displacement (MSD) of Gold-DOPE plotted against time, averaged over many particles, on the basis of trajectories recorded at time resolutions of 2 ms and 25 μ s on the surface of cultured NRK cells. The MSD calculated for each trajectory was then averaged over all the trajectories observed in a series of experiments (26 and 12 trajectories on the cell membrane at time resolutions of 2 ms and 25 μ s, shown by red and blue circles, respectively, and 17 trajectories on the liposomal membrane at a time resolution of 25 μ s, shown by purple circles) in the full timescale (x-axis) of 60 ms (*left*) and 20 ms (*right*). The keys for the 25- μ s resolution data appear to be a solid line because of the high density of points. In the right panel, a part of the MSD-t curve shown on the left (*yellow region*) is expanded in the timescale between 0 and 20 ms, showing that the analysis of diffusion at a resolution of 2 ms is not adequate for the detection of hop diffusion of DOPE in NRK cells. Here, the 2-ms resolution data are used to simulate the typical, but cutting-edge, results of the single fluorescent molecule data. Achieving both the high time resolution and the long observation period simultaneously is difficult with single fluorescent molecule methods (such as SFVI) owing to the interplay between photobleaching and the signal-to-noise ratio required for the detection of single molecules. Further developments of high-sensitivity cameras and photostable dyes are absolutely needed.

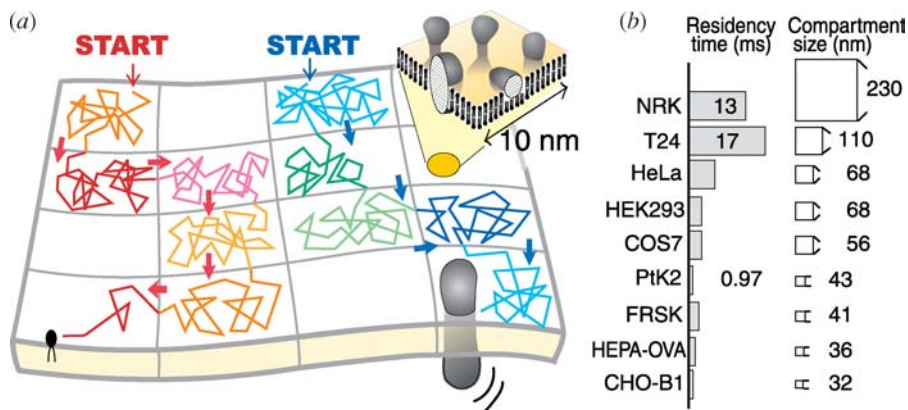


Figure 3 A paradigm shift for the plasma membrane concept is required, from the (two-dimensional) continuum fluid model to the compartmentalized fluid model, in which the membrane constituent molecules undergo short-term confined diffusion within a compartment and long-term hop diffusion between the compartments. (a) The plasma membrane is partitioned into many submicron-sized compartments with regard to the translational diffusion of membrane-incorporated molecules, and many of the molecules undergo macroscopic diffusion by repeating their confinement within a compartment and hopping to an adjacent one. The two-dimensional fluid model of Singer & Nicolson is fine if one's concern is limited to the events occurring in the membrane area limited within 10 nm (*inset*), as shown in their original cartoon. Note that in these considerations the characteristic time of the observation method or the molecular event is coupled to the space scale by way of the diffusion coefficient (microscopic or macroscopic, depending on the timescales; for the events occurring in space scales less than 10 nm, the microscopic diffusion coefficient should be used, and we recommend the value of $\approx 9 \mu\text{m}^2 \text{s}^{-1}$). As an extreme example, take the measurements of order parameters of lipid alkyl chains, using EPR spin labeling or fluorescence anisotropy decay. Both have time windows less than ≈ 10 ns, and during this period the probe would cover an area with a radius of 0.3 nm, which is comparable to the area occupied by a single alkyl chain. Thus the diffusion does not affect the measurement of the order parameter, and the order parameter at a specific point in the membrane can be observed. Such a consideration clarifies that these nanosecond-window techniques are good for revealing spatial inhomogeneities in the cell membrane, using the order parameter as a local probe. For such measurements, the Singer-Nicolson model for conceptualization is equipped to answer such questions as, How will the lipid alkyl chain order vary, depending on the distance from the transmembrane protein surface, and what happens if a lipid is sandwiched between two protein molecules? However, the Singer-Nicolson model or the two-dimensional continuum fluid model cannot be overextended to a cell membrane structure over several tens of nanometers. In these space scales, the partitioning of the plasma membrane and the hop diffusion of molecules must be considered. (b) All the mammalian cells in culture examined thus far had compartmentalized plasma membranes. The average compartment size and the average residency time within a compartment for DOPE (corrected for single molecules of DOPE using SFVI data) in various cell types are summarized. Also see Table 2.

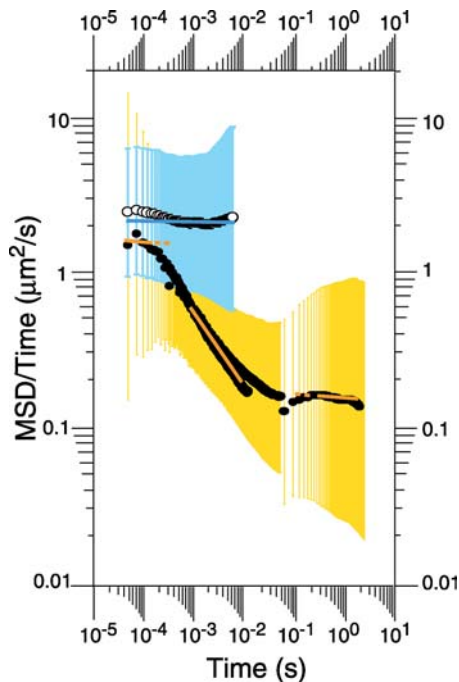


Figure 4 The plot of $\log(\text{MSD}/\text{time})$ versus $\log(\text{time})$, covering five orders of magnitude in time, obtained for gold-tagged DOPE diffusing in the plasma membrane of FRSK cells. In these cells, the average residency time within a compartment was evaluated to be 15 ms (which was then corrected for gold-induced cross-linking by using the SFVI data to give 2.3 ms), on the basis of the quantitative hop-diffusion analysis (short-term confined diffusion with occasional hops to adjacent compartments). As discussed in the text, this plot provides useful information on the changes of the diffusion characteristics that depend on the observation time intervals. The MSD of the trajectories was estimated using data obtained at time resolutions of 25 μs (5000-frames long), 110 μs (5000-frame long), and 33 ms (500-frames long) for the time windows in which the theoretically expected statistical errors in MSD are smaller than 40% (43). Then, the mean $\log(\text{MSD}/\text{time})$ values (*circles*) and their standard deviations (*colored error bars*) were plotted as a function of $\log(\text{time})$ (the MSD was estimated separately for each time resolution). In this display, simple Brownian-type diffusion is represented by a flat line (no time dependence, slope ~ 0) and anomalous diffusion is represented by a straight line with a negative slope (17, 18, 35, 54). The best fit for the data obtained for the cell membrane, assuming the three linear segments [*thick orange lines*; with α values of 0.97 (50 μs to 0.13 ms), 0.53 (1 to 10 ms), and 0.94 (300 ms to 2 s)], gives transitions at ~ 0.1 ms (or less) and between 10 and 100 ms. (Fitted regions are shown in solid lines. To help the eye, these lines are extended, as shown by broken lines. The fit between 1 and 10 ms appears to be bad, but in fact there are many more points in the lower black sequence of the closed circles.) For comparison, the plot for the trajectories in membrane blebs (*open circles*, 1000 frames; $n = 24$) and the best regression result (blue line, $\alpha \sim 1.0$) are also shown. Adapted from figure 9 in Murase et al. (35).

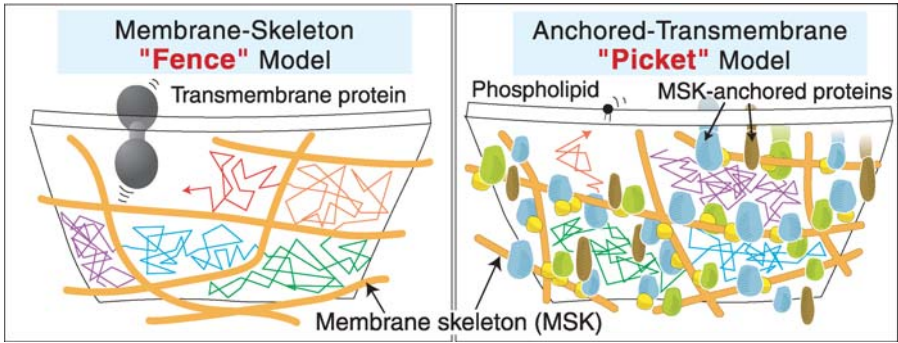


Figure 5 The models of the membrane-skeleton “fence” (*left*) and the anchored-transmembrane protein “pickets” (*right*) that together partition the entire plasma membrane into small compartments. See text for further details. The hydrodynamic friction–like effect was first described by Bussell et al. (5, 6).

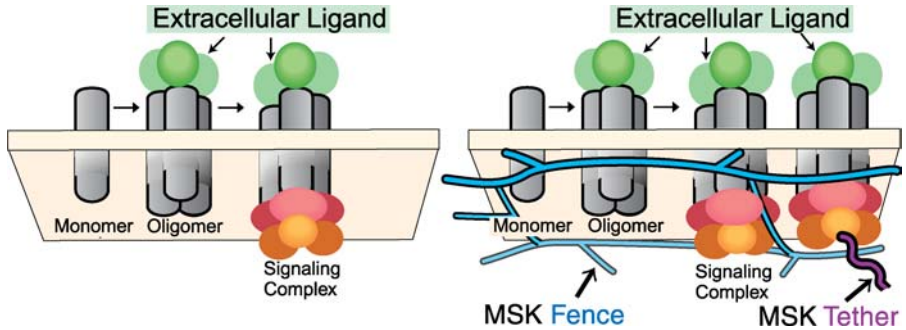


Figure 6 Oligomerization-induced trapping model showing that, upon molecular complex formation or oligomerization, membrane molecules may experience enhanced corraling and binding (tethering) by the membrane skeleton, leading to greatly reduced diffusion or immobilization. Upon oligomerization or molecular complex formation, the hop rate across the intercompartmental barrier would be greatly reduced (*right*) because, in the case of molecular complexes (in contrast to monomers), all the molecules that form the complex have to hop across the picket fence line simultaneously. In addition, owing to the avidity effect, molecular complexes are more likely to be tethered to the membrane skeleton, perhaps temporarily, which also reduces their overall diffusion rate. These enhanced confinement and binding effects induced by oligomerization or molecular complex formation are collectively termed oligomerization-induced trapping (23). This would not occur in the absence of membrane-skeleton fences and pickets (*left*): The diffusion theory by Saffman & Delbrück (45), based on the fluid mosaic model of Singer & Nicolson (69), predicts that the diffusion rates of the oligomeric complexes would be almost identical to those of the single-receptor molecules.

Copyright of Annual Review of Biophysics & Biomolecular Structure is the property of Annual Reviews Inc. and its content may not be copied or emailed to multiple sites or posted to a listserv without the copyright holder's express written permission. However, users may print, download, or email articles for individual use.

Copyright of *Annual Review of Biophysics & Biomolecular Structure* is the property of Annual Reviews Inc. and its content may not be copied or emailed to multiple sites or posted to a listserv without the copyright holder's express written permission. However, users may print, download, or email articles for individual use.